

## Prediction of shear-wave log in Western Canadian Sedimentary Basin (WCSB)

A. Nassir Saeed, Laurence R. Lines, and Gary F. Margrave

### ABSTRACT

Predictions of shear-wave logs in wells that do not have dipole Sonics are challenging, particularly in heavy oil reservoirs. In this study, we utilized linear-regression, robust locally weighted scattering and smoothing (LOWESS), and several other approaches of iteratively re-weighted linear least- squares inversion (IRLS) techniques to estimate shear-wave logs. The developed computer codes were implemented using well logs from three different types of reservoirs (conventional oil, heavy oil, and tight shale oil) in WCSB. The proposed methods guard against outliers, and have shown improvements in predicting shear-wave sonic logs compared to standard linear relationships (Castagna et al., 1985).

### INTRODUCTION

The general approach for estimating shear-wave log is to use empirical relationship (Castagna et al., 1985; Han et al. 1986). Linear regression is another method that locally derives empirical Castagna's constants. However, linear regression method usually influenced by the presence of outliers that might give inaccurate estimation of the slope and intercept points; thus erroneous predicted data. The weighted regression method (Saeed et al., 2010a) is another technique used to predicted shear-wave sonic log that is less influences by noise, and it guards against outliers.

### EMPRICAL MUDROCK LINE ESTIMATION

The Castagna's mud-rock line equation (Castagna et al., 1985) is written as

$$V_p = 1.16V_s + 1.36 \quad (1)$$

where sonic velocities are in *Km/sec*.

Han et al., (1986) has also established another empirical relationship used to predict shear-wave log, and is written as:

$$V_s = 0.7936V_p - 0.7868 \quad (2)$$

## PREDICTION OF SHEAR-WAVE IN WCSB

In this study, three different methods are implemented to predict shear-wave log using well logs from three different types of reservoirs (conventional oil, tight shale oil and heavy oil,) in WCSB. These methods are linear-regression; robust locally weighted scattering and smoothing, LOWESS (Cleveland, 1979), and iteratively re-weighted linear least- squares inversion (IRLS) techniques to estimate shear-wave logs.

### Conventional oil reservoir

Figure (1) shows  $V_p$ ,  $V_s$ , and  $V_p/V_s$  logs of a well from conventional oil reservoir in Blackfoot area, Alberta. The Blackfoot field represents a common style of stratigraphic trap in the Western Canadian Basin (Pendrel et. al, 1999). The producing formation is from channel sand (Glaucconitic of the Lower Cretaceous age) deposited as incised valley-fill sediments above the Mississippian carbonates (Wood and Hopkins 1992).

Figure (2) shows a cross-plot of  $V_p$  versus  $V_s$  logs where Mudrock lines represent predicted shear wave using different methods are superimposed. Furthermore, the scatter points are colored using Gamma log where sand usually has low gamma ray values. Values of the dipole sonic logs for the productive sand channel (black dots) reservoir are superimposed in the section as well. Figure (3) shows measured and predicted shear logs using ARCO equation, linear regression, and weighted regression method, LOWESS respectively. Predicted curves using the linear and weighted regression methods match the measured shear-wave log. Figure (4) shows percentages of residual for the three methods used in predicting shear-wave log of a well from conventional oil reservoir. Notice that the residual is higher for ARCO compared to regression method.

In figure (5), the Mudrock line calculated by the robust locally weighted scattering smoothing (LOWESS) method (Cleveland, 1979) can be used as a direct indicator of hydrocarbon (Saeed et al, 2010a). The mud-rock line estimated by LOWESS method has successfully delineated channel sand, whereas linear regression and ARCO mud-rock equation did not. Furthermore, the carbonate line can be easily distinguished by the LOWESS method, where it starts from the intersection point of  $V_s$  (around 2.8 Km) and  $V_p$  of 4.8Km/sec and above.

### Tight shale oil reservoir

Figure (6) shows P-wave velocity, S- wave velocity, density and Gamma ray of a well from tight shale reservoir in northern Alberta. Many oil companies have been actively targeting the Monteny formation as well as Duvernay shale. The tight light oil of shale reservoir is emerging as an important new source of energy in North America. With successful development of unconventional shale reservoir, attention has now shifted to the Duvernay shale in Alberta.

Figure (7) shows measured and predicted shear-wave logs using linear best fit, LOWESS method, ARCO and Han's empirical equations. Notice that LOWESS method

show excellent resemblance of the actual measured shear-wave log compared to predicted logs using empirical relationship.

The iteratively re-weighted least square inversion, IRLS, refines estimated model parameters as the algorithm converging to final solution. In this inverse scheme, constraints can be incorporated in either model space or data space or in both spaces. The latter is often referred as blocky inversion ((Wolke and Schwetlick, 1988).

Figure (8) shows measured and predicted shear wave log from implementing compactness constraint in the model space of the least-squares inversion (Last and Kubik, 1983; Saeed et al., 2010 b). In figure (9), the annealing M-estimator constraint (Li, 1996; Saeed et al., 2010c) is applied in data space. In general, the predicted shear-wave logs from the iteratively re-weighted least square inversion are in agreement with actual measured shear log.

### **Heavy oil reservoir**

Figure (10) shows  $V_p$ ,  $V_s$ ,  $V_p/V_s$  and density logs from a heavy oil reservoir in Pikes Peak area, Saskatchewan. The heavy oil is produced from the sands of Waseca formation of the Lower Cretaceous Mannville Group (Watson, 2004). The Pikes Peak field itself is located on an east-west structural high within an incised valley-fill channel complex (Sheppard et al., 1998).

Figure (11), shows measured and predicted shear-wave logs using linear regression, LOWESS method and empirical ARCO Mudrock empirical relationship. Notice that although predicted curve of LOWESS method has matched measured log fairly well for top through McLaren formation, however, the residual between two curves is noticeable at Waseca formation, compared to local regression and ARCO method.

## **CONCLUSIONS**

The robust locally weighted smoothing scattering method successfully maps the productive sand reservoir in conventional oil reservoir. The constraints used in the iteratively re-weighted least-squares inversion improves predicted shear-wave log of tight shale reservoir, and converges towards final solution in few numbers of iterations.

Although, the predicted shear-wave log of well in heavy oil reservoir shows a close matching to the measured shear-wave log from the top until depth where Waseca formation manifest, however, residual between measured and predicted shear grows noticeably at the zone of interest. Therefore, it's worth trying to use constraints that were implemented in tight shale reservoir or utilize multi-regression method in order to improve the accuracy of predicted shear-wave log in heavy oil reservoir.

## ACKNOWLEDGEMENTS

The authors would like to thank all of CREWES sponsors for supporting this study.

## REFERENCES

Castagna, J. P. Batzle, M.L. and Eastwood, R.L., 1985, Relationships between compressional-wave and shear-wave velocities in elastic silicate rocks: *Geophysics*, 50, 571-581.

Cleveland, W.S., 1979, Robust locally weighted regression and smoothing scatterplots: *Journal of the American Statistical Assoc.*, 74, 829-836.

Han, D. and Nur, A., and Morgan, D., 1986, Effects of porosity and clay content on wave velocities in sandstones: *Geophysics*, 51, 2093-2107.

Last, B.J., and Kubik, K., 1983, Compact gravity inversion: *Geophysics*, **48**, 713-721.

Li, S.Z., 1996, Robustizing robust M-estimation using deterministic annealing: *Pattern Recognition*, **29**, 159-166.

Pendrel, J., Stewart, R.R., Dufour, J., Goodway, B., and Van Riel, P., 1999, Offset Inversion of the Blackfoot P-wave Data and Discrimination of Sandstone and Shales: Annual Mtg. Canadian Soc. of Expl. Geophys, 52, 289-300.

Saeed, A.N., Lines, L.R., and Margrave, G.F., 2010a, Mud-rock line estimation via robust locally weighted scattering smoothing method: CREWES report, **22**.

Saeed, A.N., Lines, L.R., and Margrave, G.F., 2010b, Iteratively re-weighted least squares inversion for the estimation of density from well logs: part one: CREWES report, **22**.

Saeed, A.N., Lines, L.R., and Margrave, G.F., 2010c, Iteratively re-weighted least squares inversion for the estimation of density from well logs: part two: CREWES report, **22**.

Sheppard, G.L., Wong, F.Y. and Love, D., 1998, Husky's success at the Pikes Peak Thermal Project: Unitar Conference, Beijing, China, Expanded Abstracts.

Watson, I.A., 2004, Integrated geological and geophysical analysis of a heavy-oil reservoir at Pikes Peak, Saskatchewan: MS.c. thesis, university of Calgary.

Wolke, R., and Schwetlick, H., 1988, Iteratively re-weighted least squares algorithms, convergence analysis, and numerical comparisons: *SIAM Journal of Scientific and statistical computation*, **9**, 907-921.

Wood, J.M., and Hopkins, J.C., 1992, Traps associated with paleo-valleys and interfluves in an unconformity bounded sequence: Lower Cretaceous Glauconitic Member, Southern Alberta, Canada: *The American Association of Petroleum Geologists Bulletin*, 76, 904-926.

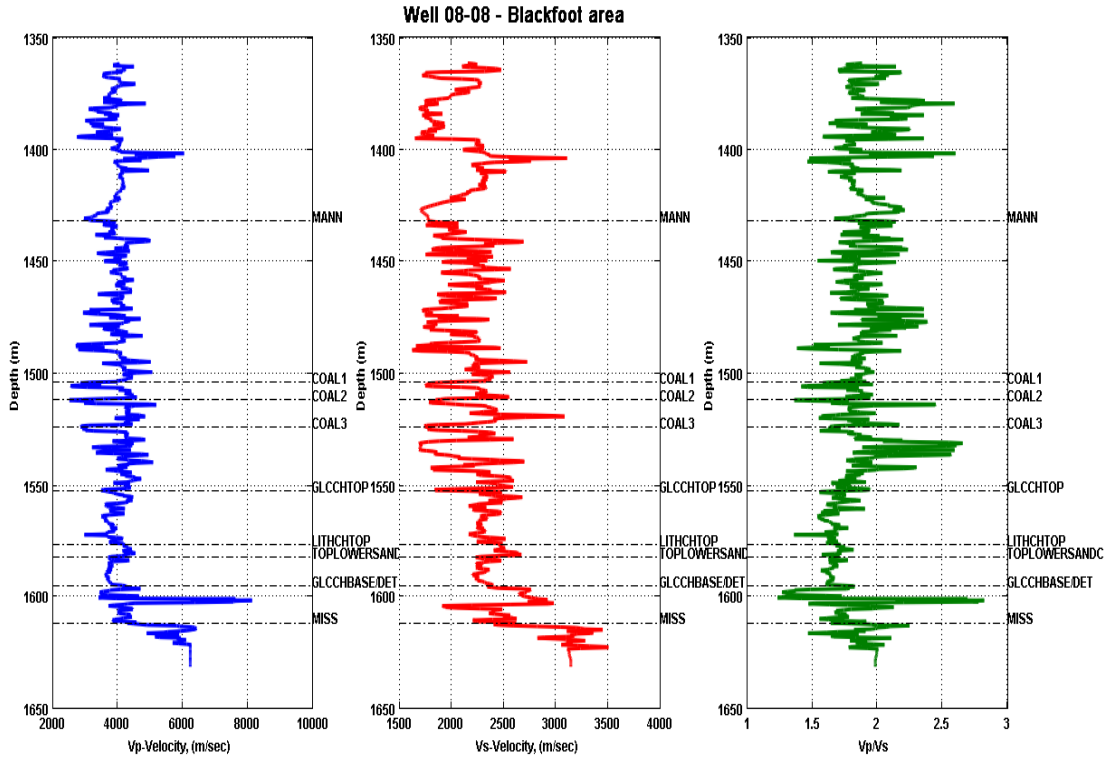


FIG.1. Plots for P-wave, S-wave and Vp/Vs logs of a well from conventional oil reservoir area.

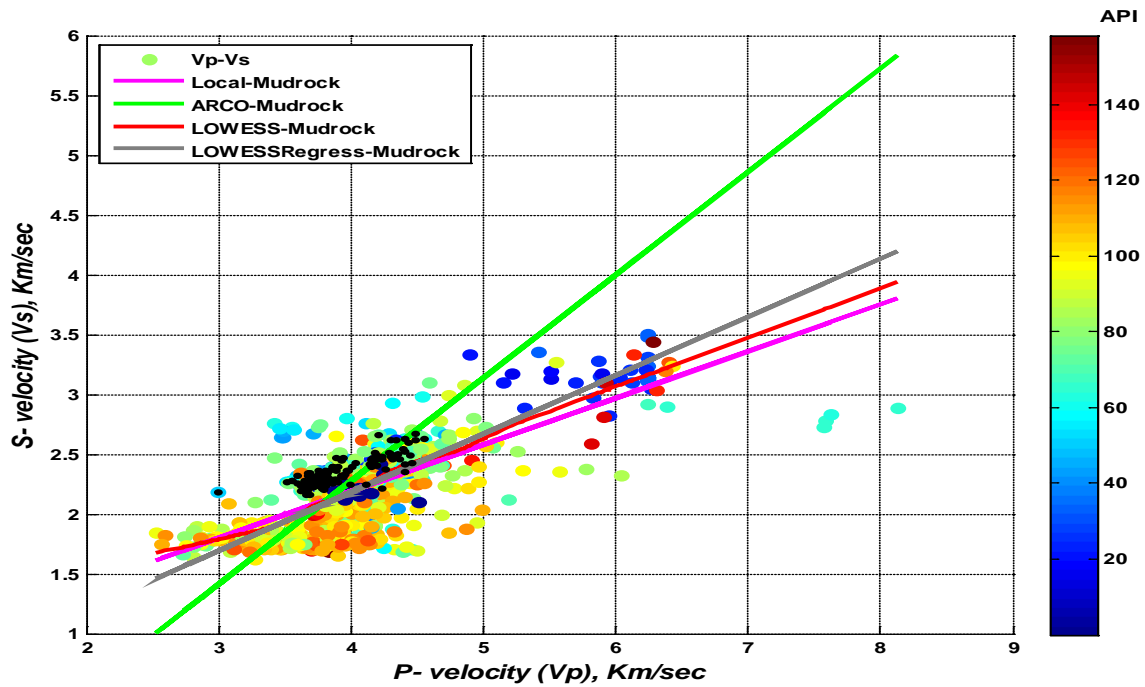


FIG.2. Cross- plot of P-wave velocity versus S-wave velocity of well log from conventional oil reservoir area. The scatter points are colored using Gamma ray. Vp-Vs values from the productive sand channel reservoir (black dots) are superimposed.

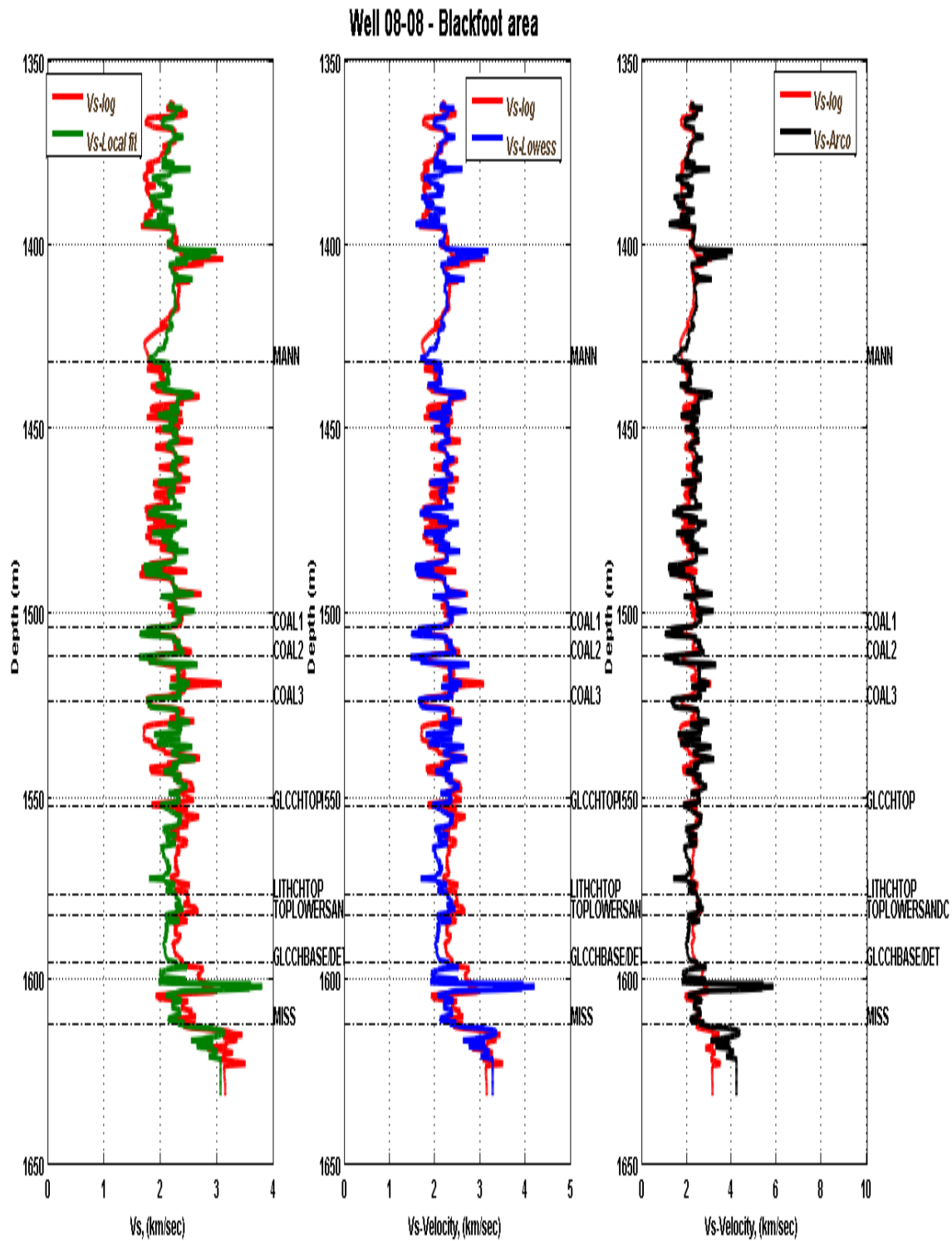


FIG.3. Plots for measured (red color) and predicted shear-wave logs of a well from conventional oil reservoir area using linear regression (green curve), LOWESS method (blue curve) and ARCO Mudrock equation (black curve).

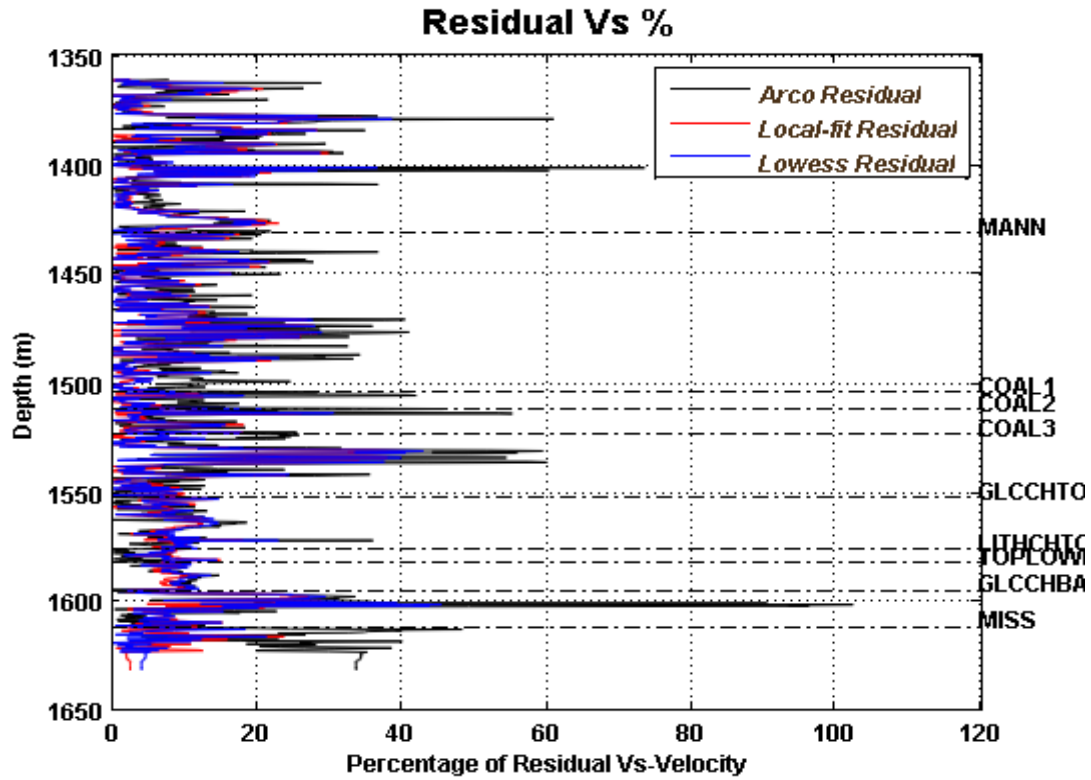


FIG.4. Plots for percentage of residual of shear-wave logs using well log from conventional oil reservoir.

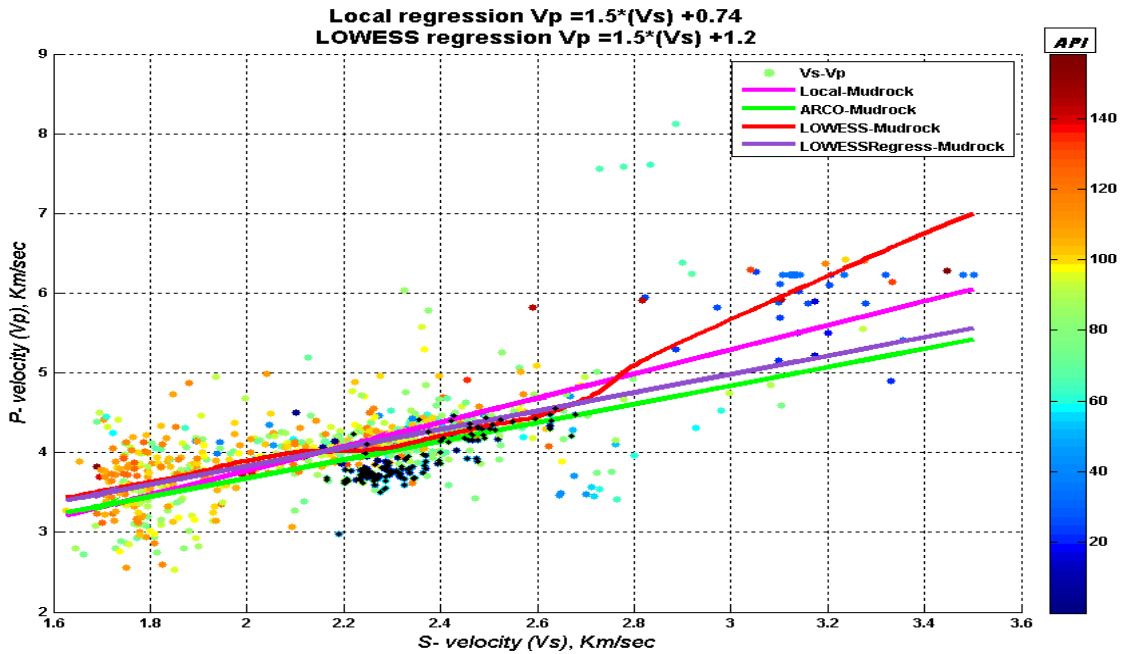


FIG.5. Cross- plot for S-wave velocity versus P-wave velocity of well log from conventional oil reservoir area. The scatter points are colored using Gamma ray, and velocity values from the productive sand channel reservoir (black dots) are superimposed.

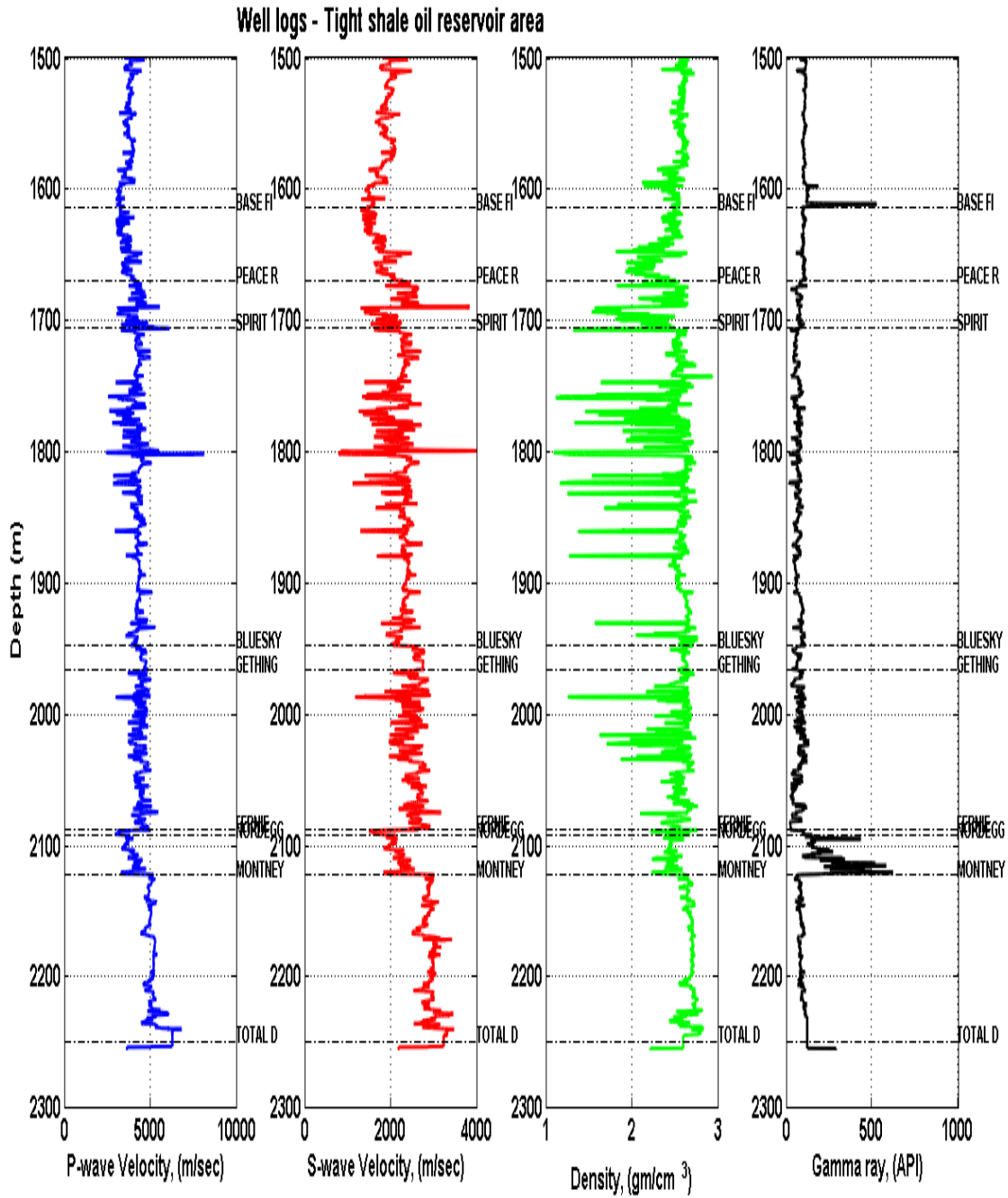


FIG.6. Plots for P-wave, S-wave, density and Gamma ray logs of a well from tight shale reservoir area.



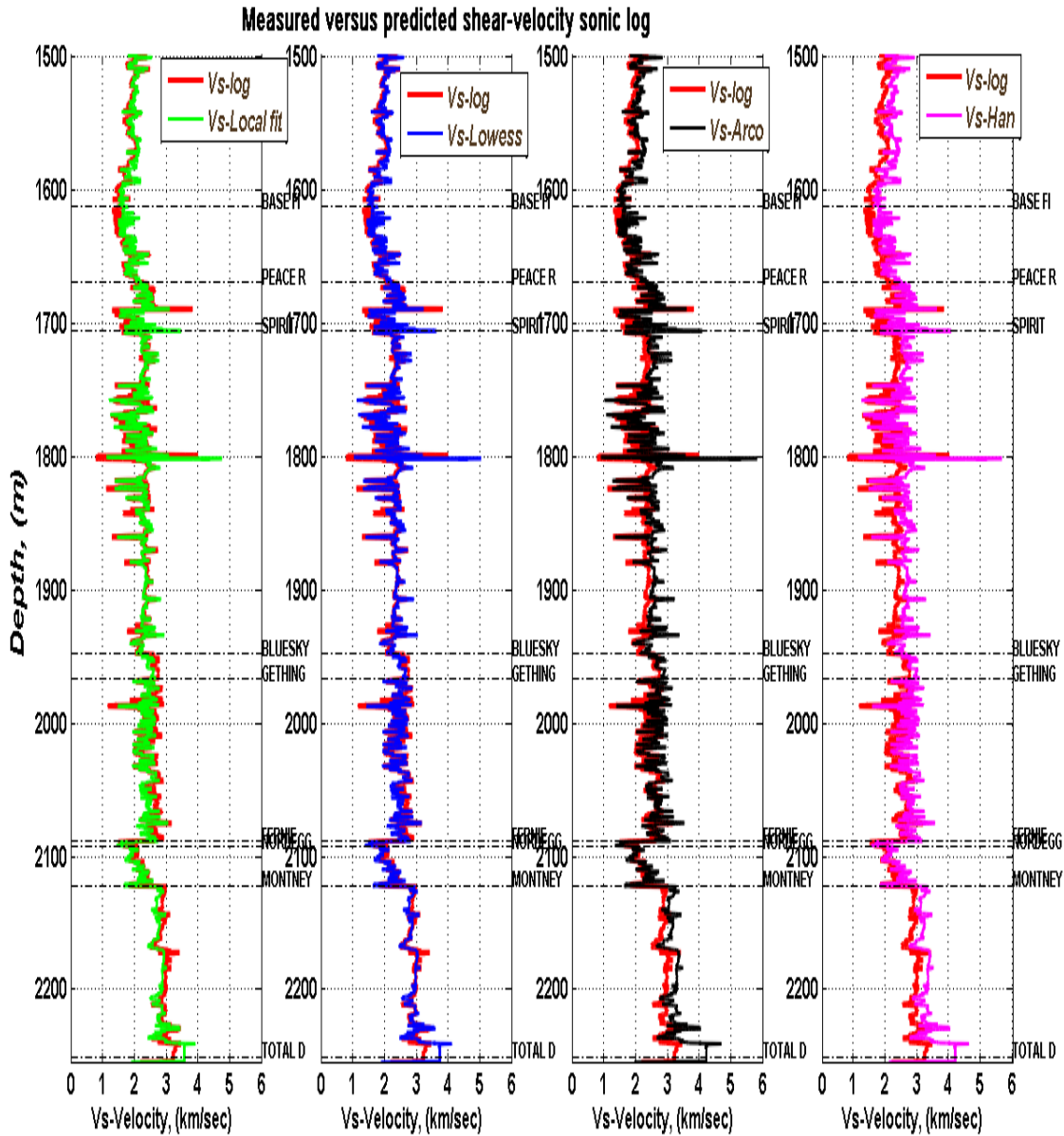


FIG.7. Plots for measured (red color) and predicted shear-wave logs of well log from tight shale oil reservoir area using linear regression (green curve), LOWESS method (blue curve), ARCO Mudrock equation (black curve) and Han's equation (magenta curve).

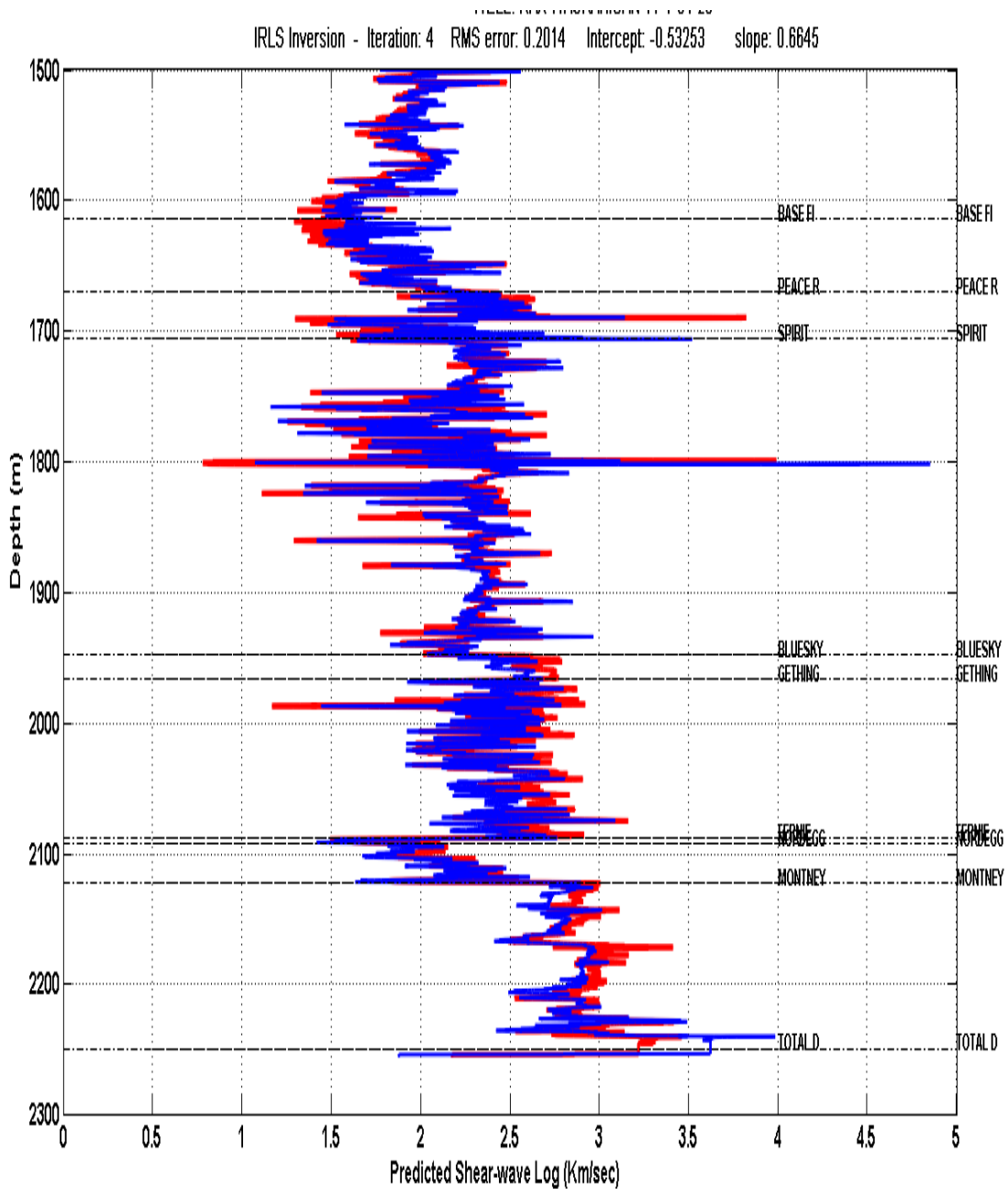


FIG.8. Measured (red color) and predicted shear-wave (blue color) logs of well log from tight shale oil reservoir area. Compactness constraint incorporated in the model space of IRLS method.

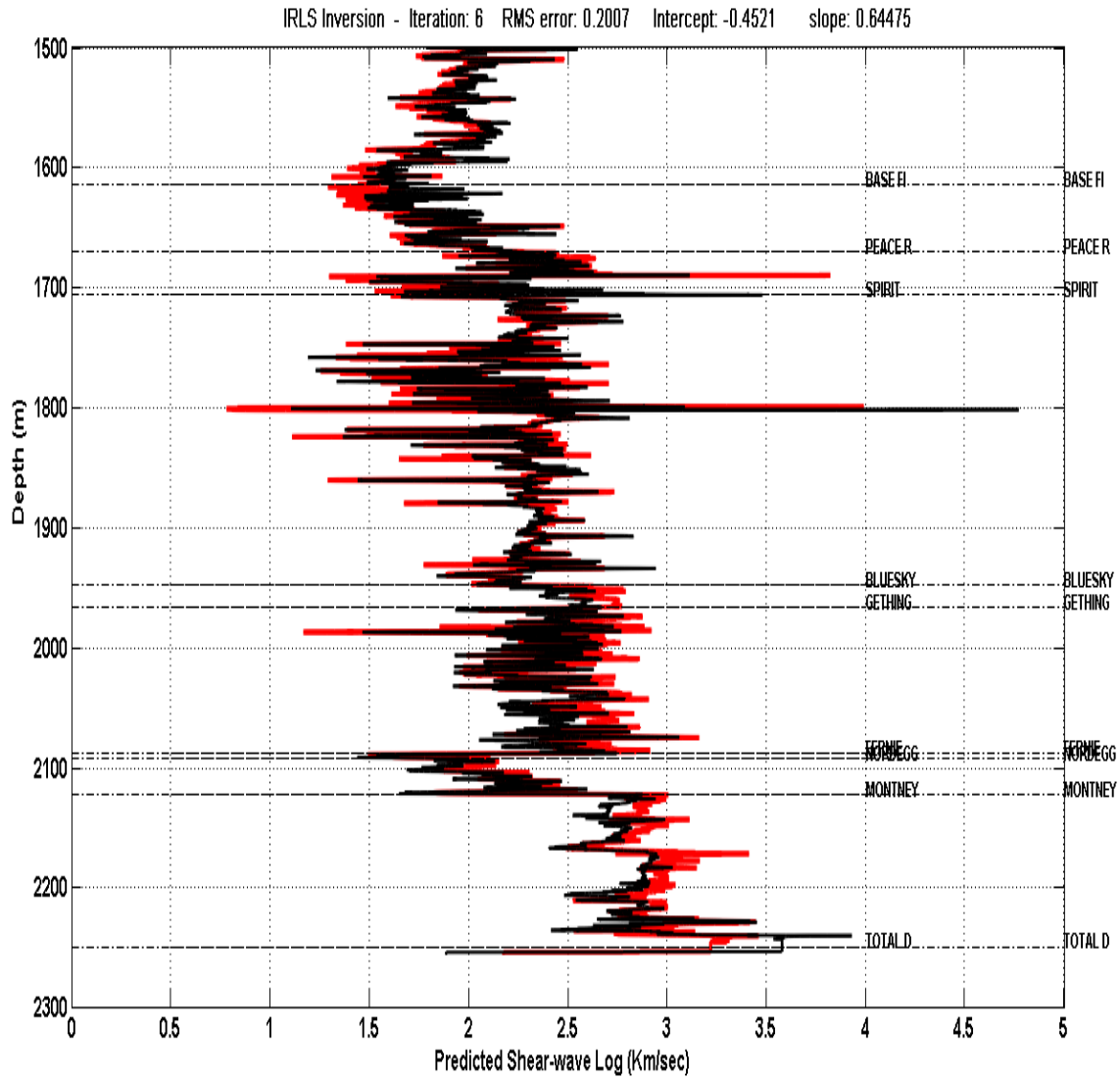


FIG.9. Measured (red color) and predicted shear-wave (black color) logs of well log from tight shale oil reservoir area. Annealing M-estimator constraint incorporated in the data space of IRLS method.

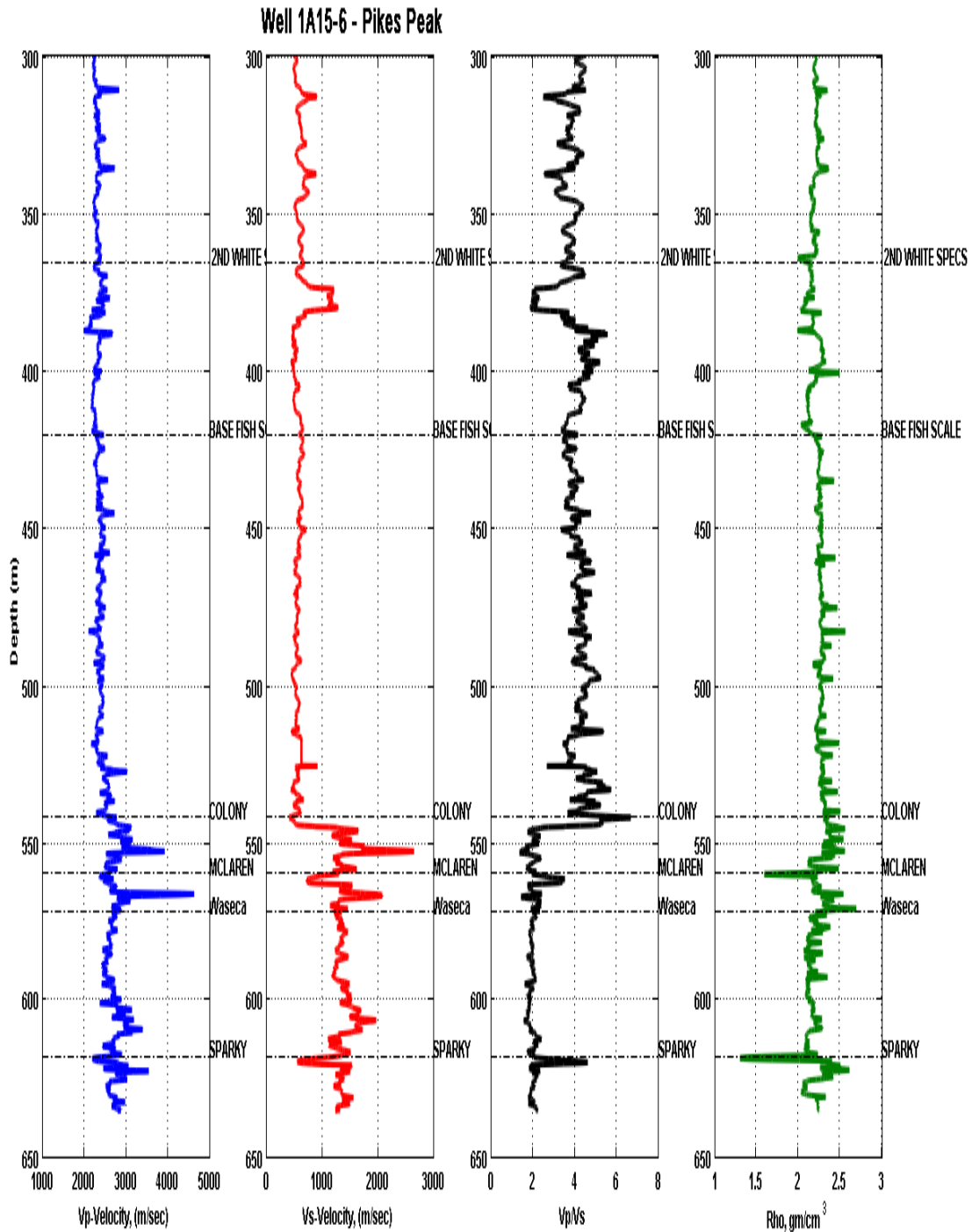


FIG.10. Plots for P-wave, S-wave, Vp/Vs and density logs of well from heavy oil reservoir.

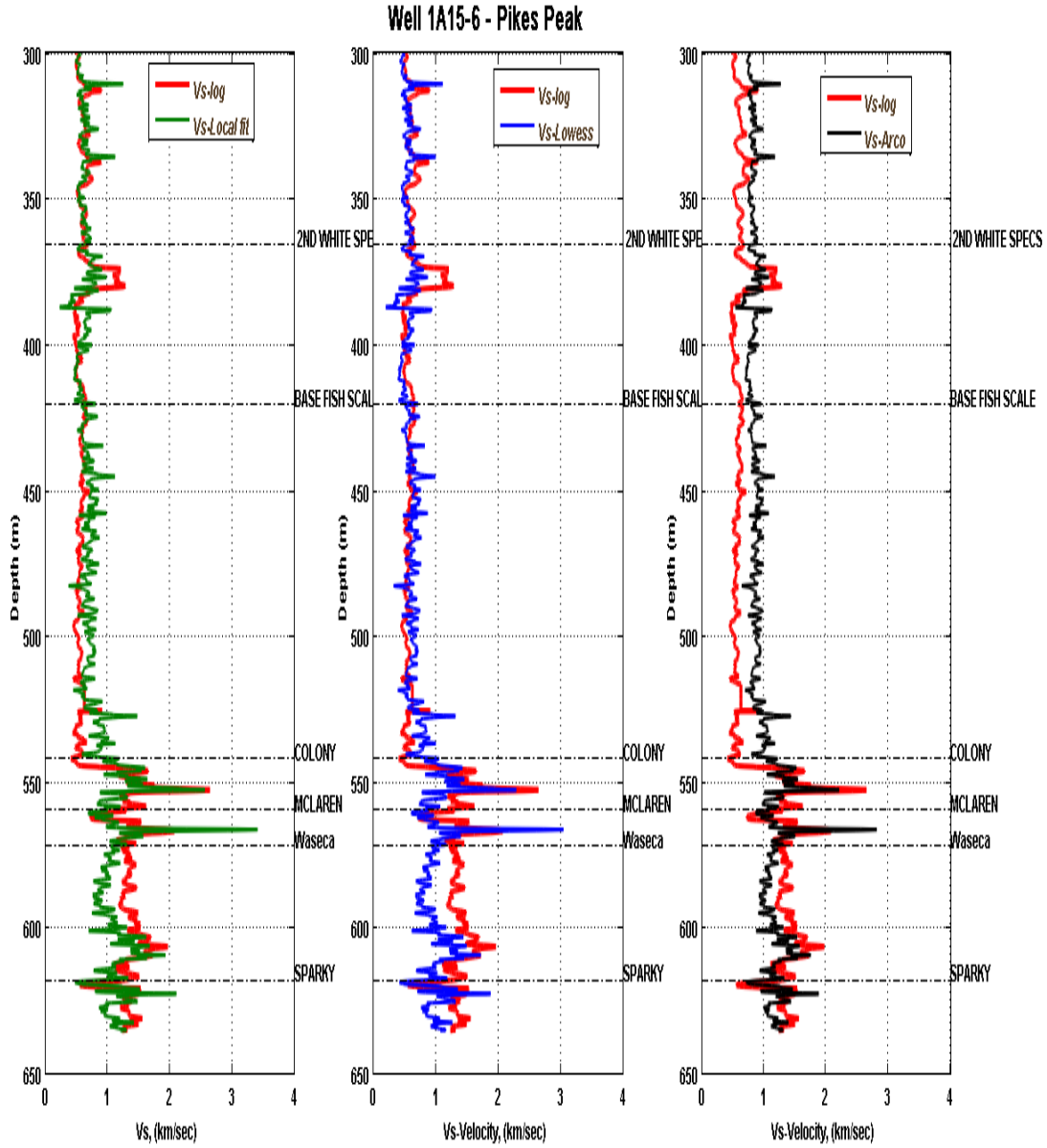


FIG.11. Plots for measured (red color) and predicted shear-wave logs of well log from heavy oil reservoir area using linear regression (green curve), LOWESS method (blue curve) and ARCO Mudrock equation (black curve).